

Harnessing the Antioxidant, Anti-Inflammatory, and Neuroprotective Potential of *Fagonia arabica*'s Biogenic Gold Nanoparticles in SK-N-SH Neuroblastoma Cells

Ibrahim Ahmed Shaikh^{1,2}, Hanish Singh Jayasingh Chellammal^{1,3}, Noordin Othman^{4,5}, Basheerahmed Abdulaziz Mannasaheb^{1,6}, Gurmeet Kaur Surindar Singh^{1,3*}

¹Department of Pharmacology and Life Sciences, Faculty of Pharmacy, Universiti Teknologi MARA, Puncak Alam, Selangor, Malaysia, ²Department of Pharmacology, College of Pharmacy, Najran University, Najran, Saudi Arabia, ³Brain Degeneration and Therapeutics Group, Universiti Teknologi MARA, Puncak Alam, Selangor, Malaysia, ⁴Department of Pharmacy Practice, College of Pharmacy, Taibah University, Al-Madinah Al-Munawwarah, Saudi Arabia, ⁵Department of Clinical Pharmacy, School of Pharmacy, Management and Science University, Shah Alam, Malaysia, ⁶Department of Pharmacy Practice, College of Pharmacy, AlMaarefa University, Diriyah, Riyadh, Saudi Arabia

Abstract

Aims: The biogenic synthesis and characterisation of gold nanoparticles (AuNPs) made from the aqueous extract of *Fagonia arabica* plant were investigated in this work, as well as their antioxidant, anti-inflammatory, and neuroprotective potential. **Materials and Methods:** The dried plant material underwent successive solvent extraction. The resulting crude extracts were subjected to standard phytochemical analyses, and the aqueous extract was further subjected to quantitative analysis for total phenols and flavonoids. The synthesized AuNPs were characterized using Fourier Transform Infrared Spectroscopy, ultraviolet-visible, X-ray diffraction, energy-dispersive X-ray (EDX), prostate-specific antigen, scanning electron microscopy, and zeta potential analysis. The *in vitro* anti-inflammatory activity was assessed using cyclooxygenase-2 (COX-2) inhibition and protein denaturation assays. Whereas the 2,2-Diphenyl-1-picrylhydrazyl (DPPH) assay was employed to determine the antioxidant activity. Cytotoxicity was tested on the L929 cell line, whereas the *in vitro* neuroprotection assessment was done on the SK-N-SH cell line. The data were provided as mean \pm standard error of the mean, and a statistical analysis was performed by a two-tailed unpaired *t*-test. **Results:** The phytochemical analysis of the extracts identified flavonoids, alkaloids, and phenols. The aqueous extract's total phenol and flavonoid content was found to be 2450.35 μ g gallic acid equivalent/g and 1980.29 μ g quercetin equivalent (QE)/g, respectively. The AuNPs were successfully characterized using various techniques, confirming their stability and optimal characteristics. The AuNPs showed crystalline nature, an average size of 111.4 nm, and a zeta potential value of -2.1 mV. The EDX analysis confirmed the presence of gold with an atomic weight of 27.5%. *In vitro* assays showed potent anti-inflammatory activity by protein denaturation (IC_{50} 118.65 μ g/mL), COX-2 inhibition (IC_{50} 109.67 μ g/mL); antioxidant activity confirmed by DPPH scavenging assay (IC_{50} 115.01 μ g/mL). Furthermore, the AuNPs exhibited minimal toxicity on normal L929 cell lines (IC_{50} 246.57 μ g/mL), indicating good biocompatibility. Notably, the AuNPs showed significant ($P < 0.001$) neuroprotective activity against trimethyltin-induced neurotoxicity in SK-N-SH neuroblastoma cells with cell viability of 78.53% at a 50 μ g/mL dose, compared to cisplatin (cell viability 13.35%). **Conclusion:** These findings suggest that *F. arabica*-synthesized AuNPs hold promise for neuroprotective applications, potentially offering new therapeutic avenues for neurodegenerative disorders. Future studies may investigate the mechanisms underlying the neuroprotective potential and assess the clinical usefulness of these nanoparticles in relevant *in vivo* models.

Key words: Alzheimer's disease; anti-inflammatory; antioxidant; *Fagonia arabica*; gold nanoparticles

Address for correspondence:

Gurmeet Kaur Surindar Singh, Department of Pharmacology and Life Sciences, Faculty of Pharmacy, Universiti Teknologi MARA, Selangor, Malaysia.
E-mail: gurmeet9952@uitm.edu.my

Received: 14-08-2025

Revised: 22-09-2025

Accepted: 28-09-2025

INTRODUCTION

Dementia is a generic word that denotes a substantial deterioration in cognitive function that disrupts an individual's daily activities. The most common kind of dementia, affecting at least two-thirds of dementia cases in those 65 and older, is Alzheimer's disease (AD). The neurodegenerative disease AD is typified by a slow onset and a steady decline in cognitive and behavioral functioning. Memory, comprehension, speaking, focus, reasoning, and judgment are all included in these functions.^[1] More than 55 million individuals globally experience dementia, with AD accounting for 60–70% of these cases.^[2]

The economic burden is equally staggering, with current costs estimated at 412 billion US\$ annually in the U.S., expected to surpass \$1 trillion by mid-century.^[3] Despite the availability of several marketed drugs, including acetylcholinesterase inhibitors (donepezil) and N-methyl-D-aspartate (NMDA) receptor antagonists (memantine), these treatments offer only symptomatic relief but do not alter the underlying cause.^[3] The currently available therapeutic choices for AD exhibit poor efficacy and limitations, emphasizing immediate attention toward developing novel pharmaceuticals for AD.^[4]

In recent years, plant-derived phytochemicals have gained significant recognition for their therapeutic benefits and potential health advantages. Their strong antioxidant and anti-inflammatory properties are vital for counteracting the harmful effects of free radicals, oxidative stress, and inflammation on neurons.^[5] Another promising avenue involves the use of nanoparticles in the management of neurodegenerative disorders. Green-synthesized nanoparticles have emerged as promising alternatives in the management of brain disorders.^[6] Among these, gold nanoparticles (AuNPs) have gained significant attention due to their special ability to cross the Blood-brain barrier (BBB) and their potential to enhance drug concentrations in the brain, making them a valuable tool in the treatment of neurological conditions.^[7]

This research concentrates on the synthesis of AuNPs using aqueous extract of *Fagonia arabica*, a plant known for its medicinal properties. *F. arabica* is highly regarded in Indian folk medicine for its numerous medical benefits. It possesses antioxidant, anti-inflammatory, neuroprotective, and anticancer potential.^[8] It is rich in phytochemicals such as flavonoids, triterpenoidal glycosides, and saponins, which significantly boost its antioxidant capacity, making it a valuable natural remedy.^[9]

This study is the first to investigate the synthesis of AuNPs using *F. arabica* plant extract and harness its anti-inflammatory, antioxidant, and neuroprotective potential in SK-N-SH neuroblastoma cells. By exploring the therapeutic benefits of *F. arabica* gold nanoparticles (*F. arabica*-AuNPs), this study aims the advance therapeutic options for neurodegenerative disorders, addressing the limitations of

current therapies and overcoming the hurdles of successful administration of drug delivery to the brain.

MATERIALS AND METHODS

Chemicals and consumables

We purchased gold chloride (AuCl₃) from Sigma-Aldrich, USA. The remaining chemicals were of analytical quality and acquired from Hi-media Chemicals, India.

Collection and extraction of plant material

Whole plants of *F. arabica* were collected from the Najran University Campus in Najran, Saudi Arabia, and authenticated by Prof. Mohamed A. A. Orabi (Department of Pharmacognosy) using a herbarium specimen (Fag. 1503–2021). The plant material was thoroughly washed with distilled water, shade-dried at room temperature, and ground into coarse powder (mesh size 30). The powdered sample was stored at –20°C in sealed containers for future use. For extraction, the soxhlet extraction technique was employed using successive solvents – hexane, ethyl acetate, ethanol, and distilled water. For the Soxhlet extraction, solvent ratio of 1:10 was selected and each solvent was subjected to 12 to 24 h of extraction. Using a rotary vacuum evaporator, the extracts were subsequently concentrated and stored at –20 for further experimental applications.^[10]

Phytochemical analysis and quantification

The crude solvent extracts of *F. arabica* were qualitatively analyzed for various phytochemical constituents using the methodology previously described.^[11] Gallic acid (GA) calibration curves were created ranging between 20 and 100 µg/mL. The GA equivalents (GAEs), which are measured as milligrams (mg) of GAE/g of dry weight, were used to standardize the extract's phenolic contents.^[12] Similarly, the concentration of total flavonoids was measured using the aluminum chloride procedure.^[13]

Synthesis of *F. arabica*-AuNPs

A preliminary pilot experiment involved the combination of 1 mL of a 1% (1 g/100 mL) aqueous extract of *F. arabica* with 10 mL of a 10 mM gold chloride solution. The reaction was carried out in the dark for 4 h, during which a color change from colorless to dark purple was observed. Subsequently, bulk synthesis of *F. arabica*-AuNPs was done as per the same ratio, mixing 40 mL of the *F. arabica* aqueous extract with 400 mL of gold chloride solution. The *F. arabica*-AuNPs were isolated by continuous centrifugation (3–4 cycles) at 10,000 rpm and 15°C. The supernatant was discarded, and the subsequent pellets were washed with deionized water and dried.^[14] The powdered *F. arabica* -AuNPs were then stored for future use.

Characterization of *F. arabica*-AuNPs

The AuNPs underwent various testing methods, including ultraviolet (UV), prostate-specific antigen (PSA), scanning electron microscopy (SEM), Fourier Transform Infrared Spectroscopy (FTIR), EDX, X-ray diffraction (XRD), and zeta potential analysis.

UV-visible (UV-vis) spectrophotometry

The gold ion reduction in the colloidal solution was verified and examined using UV-vis spectroscopy. A quartz cuvette containing a 1 mL aliquot sample was used for UV-vis scanning at a wavelength between 200 and 700 nm. The reference was distilled water, and the blank was 1 mM HAuCl₃. To perform the measurements, a Shimadzu UV-1800 spectrophotometer was used.^[15]

XRD analysis

The Shimadzu XRD-6000/6100 model was used for XRD analysis to identify the crystalline structure, size, phase nature, and lattice parameters of the AuNPs. Cu-K α radiation with a scattering 2 θ range of 20°–80° was used.^[16]

Zeta potential and PSA

The Zetasizer Nano ZS device (HORIBA SZ-100) was used to measure the particle size and zeta potential of the *F. arabica* AuNPs. Two milligrams of *F. arabica* AuNPs were dissolved in 2 mL of distilled water for 5 min. The Zetasizer electrode was then loaded with 0.5 mL of the sample using ultrasound, which was examined in a 50–800 nm range.^[17]

SEM and EDX analysis

The nature, size, shape, and surface area of the AuNPs were measured using a SEM (JEOL model number JSM-IT500L). High-resolution SEM imaging enables particle imaging, whereas EDX determines the elemental and chemical characteristics. SEM-EDX can provide information about the material's exterior morphological properties, composition, chemical makeup, and orientation. Following dehydration, the samples were analyzed with an electron beam, allowing AuNPs' size and image data to be determined.^[18]

FTIR analysis

The potassium bromide pelleting method was used to obtain the FTIR spectra, which were recorded in the wavelength range of 4000–400 cm⁻¹ at a 1:100 ratio (Model: NICOLET 6700).^[19]

In vitro biological activity of *F. arabica*-AuNPs

Protein denaturation assay

The protein denaturation method was used to assess *F. arabica*-AuNPs' anti-inflammatory capabilities and compared with the standard was aspirin.^[20] Two milliliters of bovine serum albumin were used in the experiment, incubated at 37 \pm 1°C

for 15 min. Phosphate-buffered saline (2.8 mL, pH 6.4) and 2 mL of the test sample (AuNPs) or standard (50–250 μ g/mL) made up the reaction mixture. The mixture was then incubated at 70°C to initiate denaturation of proteins. With distilled water serving as the blank, absorbance measurements were made at 660 nm. To ascertain the effectiveness, the IC₅₀ values and protein denaturation inhibition (%) were computed.

In vitro COX-2 inhibition assay

The COX Inhibitor Screening Assay Kit from Cayman Chemical, MI, USA, was used to assess the cyclooxygenase inhibitory capability of *F. arabica*-AuNPs as per the previously described procedure. The effectiveness of the compound was assessed by determining the concentration that resulted in 50% enzyme inhibition (IC₅₀).^[21]

In vitro antioxidant DPPH assay

Using a slightly altered protocol from earlier research, the antioxidant capacity of *F. arabica*-AuNPs was assessed and compared with ascorbic acid standard.^[22] Different concentrations of AuNPs and the standard (50–250 μ g/mL) were combined with 1 mL of a 0.2 mM DPPH solution. After the mixture was allowed to sit at room temperature in a dark place for 30 min, its absorbance was recorded at 517 nm.

In vitro toxicity of *F. arabica*-AuNPs in non-cancerous fibroblast cell line L929

The standard colorimetric 3-(4,5-dimethylthiazol-2-yl)-2,5-diphenyltetrazolium bromide (MTT) assay was utilized to assess the impact of AuNPs on the viability of the normal fibroblast cell line L929, following the method described previously.^[23] The dose-response curves were used to calculate the IC₅₀ values.

In vitro neuroprotective activity *F. arabica*-AuNPs in SK-S-NH cell lines

The neuroprotective activity of *F. arabica*-AuNPs was determined using SK-S-NH neuroblastoma cell lines and the MTT pre-treatment method as described previously.^[24]

Statistical analysis

An independent Student's *t*-test was employed to evaluate statistical differences between groups. It was determined that a *P* < 0.05 was statistically significant.

RESULTS AND DISCUSSION

Phytochemical analysis of *F. arabica*

The results demonstrated that the phytochemicals vary in each solvent extract, which could be attributed to

polarity differences. Hexane and ethyl acetate extracts primarily contained lipids and oils, whereas ethanol and aqueous extracts contained alkaloids, terpenoids, phenols, and flavonoids.

Quantification of total phenols and flavonoids

Based on the qualitative results, the ethanol and aqueous extracts of *F. arabica* were quantified using standard procedures for total phenols and flavonoids. The standard curve calibration was used to quantify the total phenol and flavonoid concentration. The aqueous extract had more content of total phenol (2450.35 µg GAE/g of dry weight) and flavonoids (1980.29 µg QE/g dry weight) than the ethanol extract (1450.65 µg GAE/g and 987.30 µg QE/g, respectively). Hence, as per the quantitative results, the aqueous extract was selected for the synthesis of AuNPs.

Biogenic synthesis of AuNPs

The *F. arabica* aqueous extract served as both a capping and reducing agent in the synthesis of AuNPs through the phytochemical reduction method, with 10 mM of gold chloride used as precursor solution. It reduced the gold chloride into AuNPs by changing the colorless solution to a dark purple color.

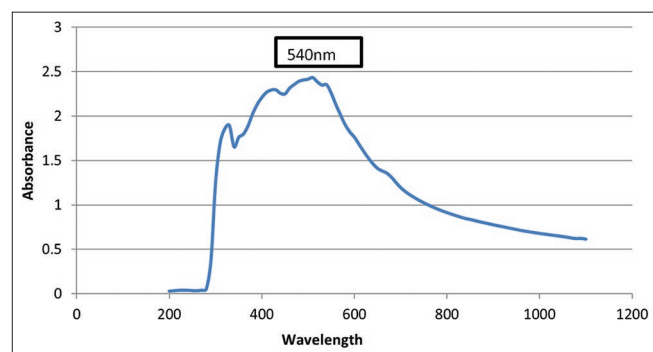


Figure 1: Ultraviolet-visible spectra of synthesized gold nanoparticles showing a characteristic peak at 540 nm

The synthesis of AuNPs using phytochemicals as reducing agents is an area of significant interest due to its potential applications in various fields, including medicine, catalysis, and electronics.^[25]

Characterization of nanoparticles

UV-vis spectral analysis of AuNPs

The UV-vis spectra are shown in Figure 1, with a prominent peak at 540 nm caused by surface plasmon resonance. It is evident from the emergence of a peak in the visible range (500–600 nm) that the aqueous extract of *F. arabica* significantly reduced the gold ions to AuNPs.

FTIR analysis

FTIR spectroscopy was employed to characterize the surface chemistry of *F. arabica*-derived AuNPs, revealing key functional groups involved in nanoparticle stabilization. The spectrum exhibited prominent peaks at 3339.29, 2126.57, 1632.49, 1389.21, 1238.19, and 1074.18 cm^{-1} , indicating the presence of various organic moieties. The broad peak at 3339.29 cm^{-1} corresponds to O–H stretching vibrations, likely from hydroxyl groups or adsorbed water molecules. The 2126.57 cm^{-1} peak suggests $\text{C}\equiv\text{C}$ or $\text{C}\equiv\text{N}$ stretching, indicative of alkyne or nitrile groups possibly originating from capping ligands. The 1632.49 cm^{-1} peak is attributed to N–H bending or $\text{C}=\text{O}$ stretching, pointing to amines or amides, which may reflect biomolecular interactions. Peaks at 1389.21 cm^{-1} and 1238.19 cm^{-1} denote C–H bending and C–O stretching, respectively, suggesting the presence of alkyl chains, carboxylates, alcohols, or ethers. The 1074.18 cm^{-1} peak further supports the presence of stabilizing agents such as surfactants or polymers [Figure 2].

XRD analysis of AuNPs

XRD analysis allows the determination of the crystal structure of AuNPs. In the case of AuNPs, XRD can confirm whether they possess the expected face-centered cubic (FCC)

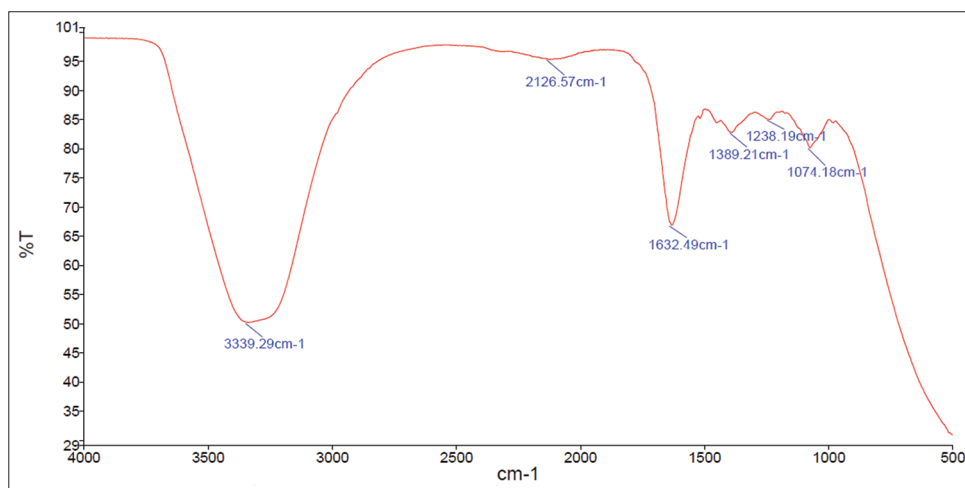


Figure 2: Fourier transform infrared spectroscopy spectra of synthesized gold nanoparticles showing various functional groups

crystal structure or if they have undergone any structural modifications during synthesis. In the present study, the diffraction pattern exhibited distinct peaks at 2θ values of approximately 38.03° , 44.13° , 64.38° , and 77.35° . The peaks were relatively sharp, indicating good crystallinity of the

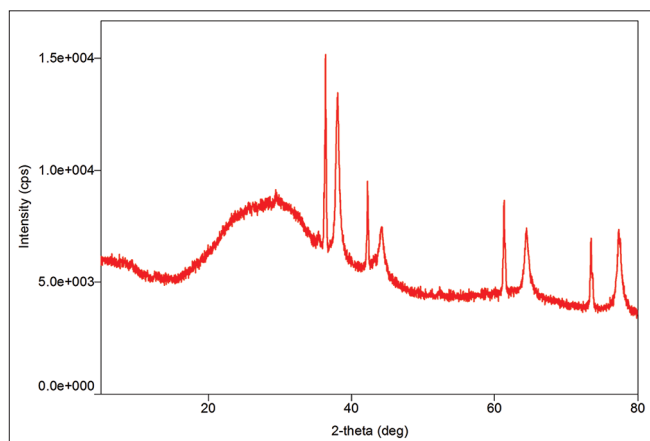


Figure 3: X-ray diffraction spectral analysis of synthesized gold nanoparticles

AuNPs. The peaks correspond to the (111), (200), (220), and (311) planes of the FCC gold crystal structure^[26] as depicted in Figure 3.

Particle size analysis

In the current study, the synthesized AuNPs exhibited an average size of 98.3 nm, as depicted in Figure 4. This indicates that the *F. arabica* AuNPs are relatively small and uniform in size, which is crucial for various applications in nanotechnology and medicine. The particle size of 98.3 nm is ideal for a wide range of applications in nanotechnology and medicine, including drug delivery and therapeutics, ensuring predictable and reliable performance and making the AuNPs highly versatile.^[27]

Zeta potential analysis of AuNPs

In the current research, the synthesized AuNPs exhibited a zeta potential value of approximately -2.1 mV [Figure 5]. This value indicates that the nanoparticles have a slight negative charge on their surface. Zeta potential is a key parameter

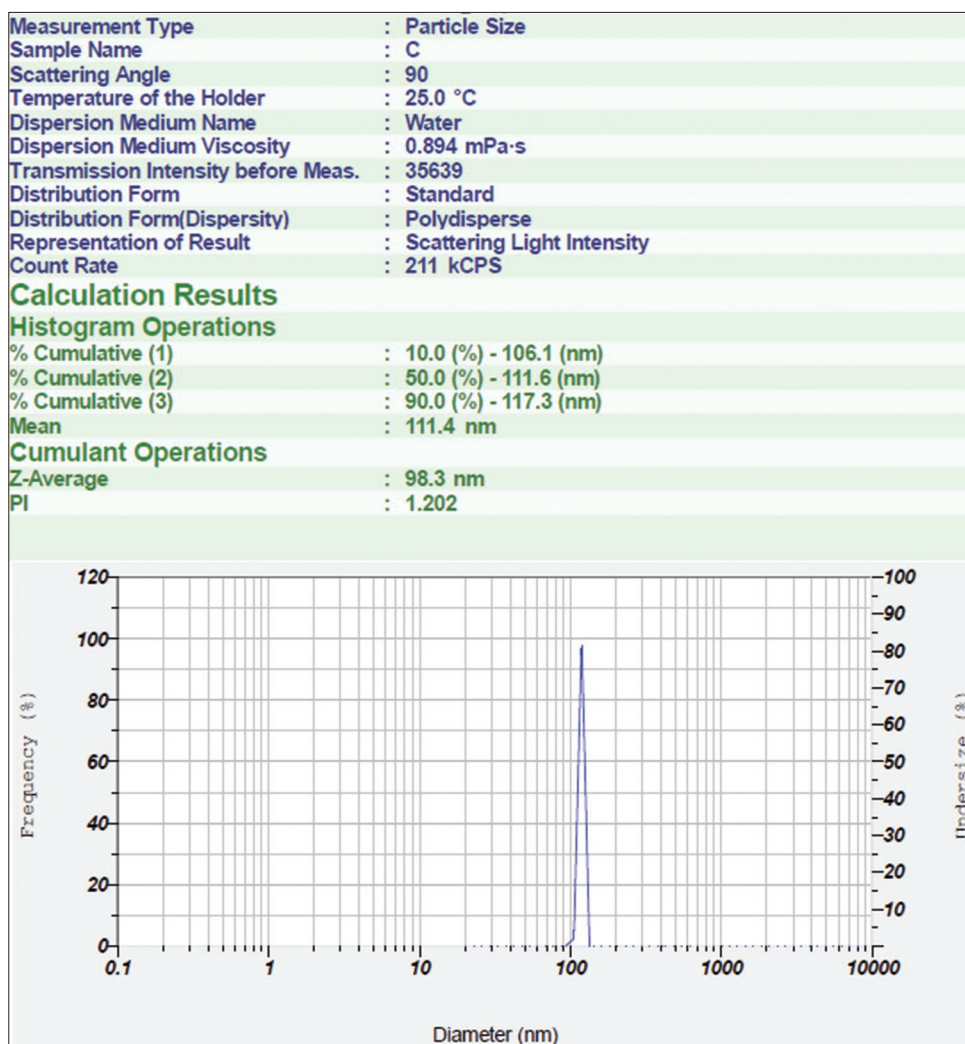


Figure 4: Particle size analysis of synthesized gold nanoparticles, revealing a Z-Average of 98.3

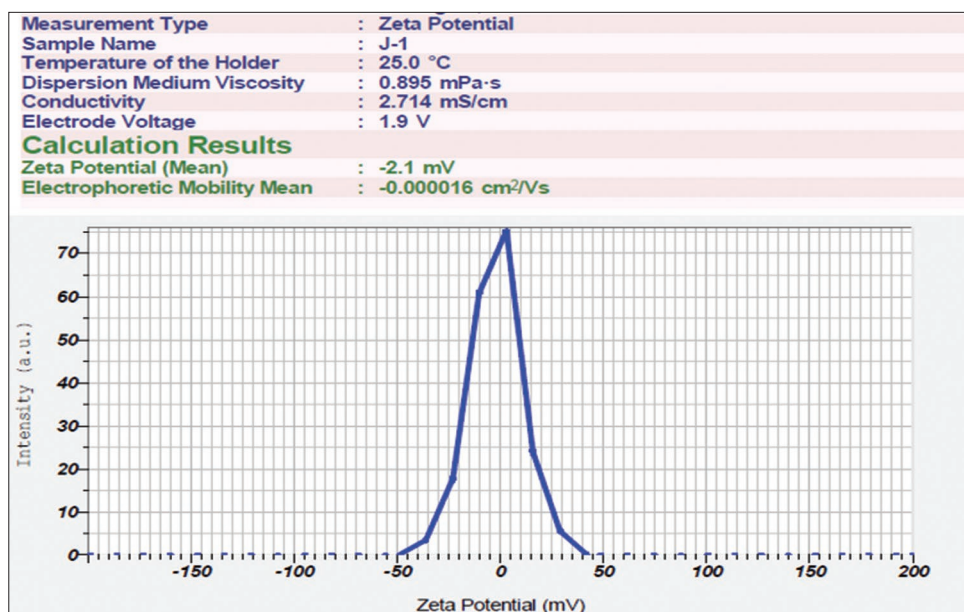


Figure 5: Zeta potential analysis of synthesized gold nanoparticles, revealing a value of -2.1 mV

in understanding the stability of nanoparticle suspensions; values close to zero suggest that the particles may have a tendency to aggregate, as there is minimal repulsive force between them. Higher zeta potential values (negative or positive) indicate stronger repulsive forces between particles, leading to increased electrostatic stabilization and reduced aggregation or flocculation.^[28]

SEM and EDX analysis

In the present study, SEM showed spherical shapes and agglomeration patterns of the particles, providing a detailed understanding of their morphological characteristics. The SEM analysis revealed the formation of spherical AuNPs with a size range of 87–200 nm [Figure 6]. SEM is a versatile imaging method that uses a high-energy electron beam to interact with the sample surface, generating a multitude of data about its topography, surface features, and nanostructure.^[29]

In addition, the EDX analysis confirmed the presence of gold with atomic weight 27.5%, by showing a sharp peak between 1 and 3 keV, indicating the AuNPs synthesis [Figure 7]. The EDX analysis confirmed the presence of oxygen and carbon, which are known for their role as capping and reducing agents.^[30]

In vitro biological studies of synthesized AuNPs

In vitro anti-inflammatory activity

The anti-inflammatory potential of *F. arabica*-derived AuNPs was assessed in comparison with aspirin at concentrations of 50 μ g and 250 μ g. At 50 μ g, AuNPs exhibited 29.87% inhibition, while aspirin showed 40.47%. Upon increasing the concentration to 250 μ g, inhibition rose significantly to 80.73% for AuNPs and 86.31% for aspirin [Table 1]. Although aspirin remained slightly more effective, AuNPs

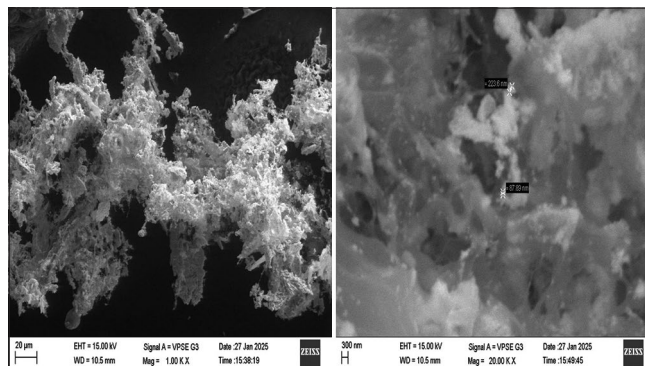


Figure 6: Scanning electron microscopy analysis of synthesized gold nanoparticles

demonstrated strong dose-dependent anti-inflammatory activity. These results align with previous studies reporting comparable IC_{50} values for protein denaturation inhibition using AuNPs synthesized from *Citrus sinensis* peel extract.^[31]

The AuNPs demonstrated strong COX-2 inhibitory activity, comparable to the standard drug mefenamic acid. At 250 μ g, AuNPs achieved 86.26% inhibition versus 91.17% by the standard. The IC_{50} values were 109.67 μ g for AuNPs and 80.78 μ g for mefenamic acid, indicating potent but slightly lower efficacy [Table 2]. These results support previous findings with *Isodon excisus*-derived AuNPs, highlighting their potential for nanomedicine-based anti-inflammatory therapies.^[32]

Antioxidant activity based on DPPH assay

At 250 μ g/mL, the AuNPs demonstrated an antioxidant activity of $84.36 \pm 0.6478\%$, whereas the standard ascorbic acid showed a comparable activity of $90.06 \pm 0.4993\%$. The IC_{50} values, which represent the concentration required to inhibit 50% of the DPPH radicals, were found to be

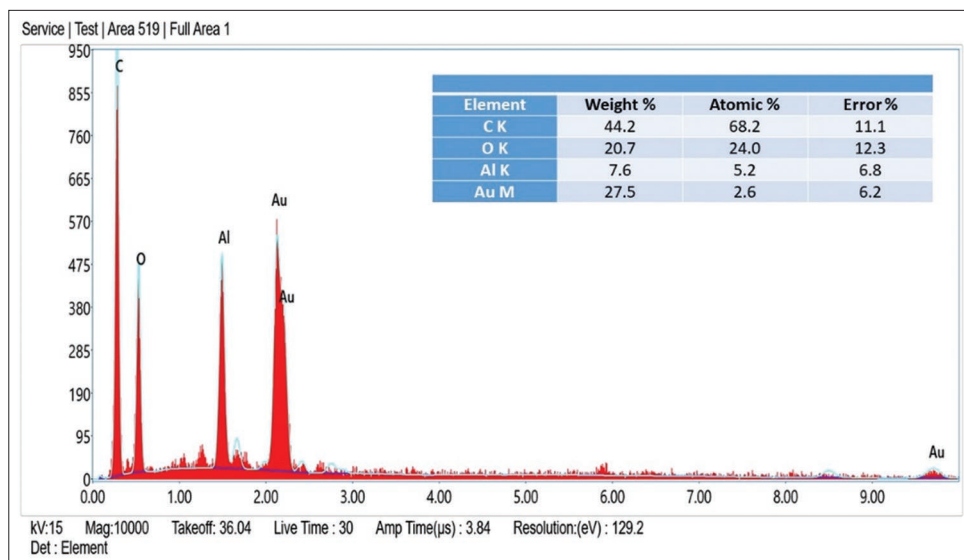


Figure 7: EDX analysis of synthesized gold nanoparticles

Table 1: Anti-inflammatory activity of AuNPs by denaturation assay

Concentration in $\mu\text{g/mL}$	<i>F. arabica</i> -AuNPs	Standard drug (Aspirin)
50	29.87 \pm 0.83	40.47 \pm 1.98
100	45.77 \pm 1.78	55.50 \pm 1.55
150	62.19 \pm 0.87	68.58 \pm 0.65
200	71.30 \pm 0.68	74.47 \pm 0.96
250	80.73 \pm 0.26	86.31 \pm 0.67
IC ₅₀ ($\mu\text{g/mL}$)	118.65	81.92

The results are expressed as mean \pm standard error. AuNPs: Gold nanoparticles

Table 2: Anti-inflammatory activity of AuNPs by COX-2 inhibition assay

Concentration (μg)	<i>F. arabica</i> -AuNPs	Standard drug mefenamic acid
50	36.48 \pm 0.55	41.89 \pm 0.73
100	47.03 \pm 0.62	56.81 \pm 0.66
150	58.41 \pm 0.38	64.75 \pm 0.66
200	72.08 \pm 0.27	78.77 \pm 0.71
250	86.26 \pm 0.63	91.17 \pm 0.47
IC ₅₀ ($\mu\text{g/mL}$)	109.67	80.78

The data are presented as mean \pm standard error of the mean. AuNPs: Gold nanoparticles

115.01 $\mu\text{g/mL}$ for AuNPs and 76.44 $\mu\text{g/mL}$ for the standard [Table 3]. Overall, the results suggest that AuNPs exhibit significant antioxidant activity, although they are slightly less effective than the standard.

There were no statistically significant differences between the AuNPs and the standard drug, according to the statistical analysis conducted using an independent Student's *t*-test

Table 3: The DPPH antioxidant activity results

Concentration ($\mu\text{g/mL}$)	<i>F. arabica</i> -AuNPs	Standard drug (Ascorbic acid)
50	32.34 \pm 0.74	45.03 \pm 0.55
100	46.72 \pm 0.42	54.13 \pm 0.48
150	61.19 \pm 0.69	66.39 \pm 1.31
200	69.86 \pm 0.60	78.65 \pm 0.48
250	84.36 \pm 0.64	90.06 \pm 0.49
IC ₅₀ ($\mu\text{g/mL}$)	115.01	76.44

The data are presented as mean \pm standard error of the mean. AuNPs: Gold nanoparticles

(unpaired two-tailed). The comparable inhibition indicates that AuNPs can be as effective as the standard drug in antioxidant and anti-inflammatory activities.^[33] The results of the current study are in line with a previous study conducted by Nagalingam *et al.*, 2018, which highlighted the production of AuNPs by employing *Alternanthera bettzickiana* extract, demonstrating their significant antibacterial, anticancer, and therapeutic properties.^[34]

Evaluation of toxicity of AuNPs on non-cancerous L929 cell line

AuNPs showed low cytotoxicity, with an IC₅₀ of 246.57 $\mu\text{g/mL}$. At 50 $\mu\text{g/mL}$, cell viability remained high (92.08%), whereas at 250 $\mu\text{g/mL}$, viability dropped to 27.81%, indicating dose-dependent cytotoxicity [Table 4]. Microscopic analysis revealed normal morphology at lower doses, whereas higher concentrations caused cell deformation and death, similar to cisplatin-treated cells [Figure 8]. These results suggest that AuNPs are biocompatible at low doses but exhibit cytotoxic effects at higher concentrations.^[35]

Overall, the statistical analysis using the unpaired *t*-test (two-tailed) reveals the considerable cytotoxic effects of AuNPs

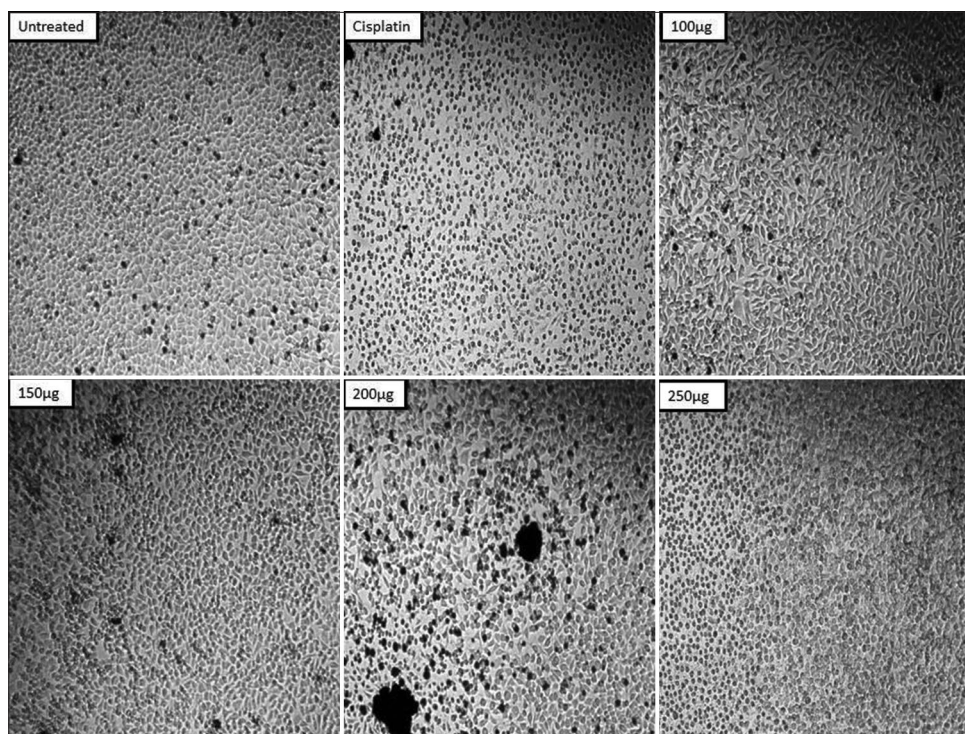


Figure 8: Morphological effects of gold nanoparticles against the L929 fibroblast cell line

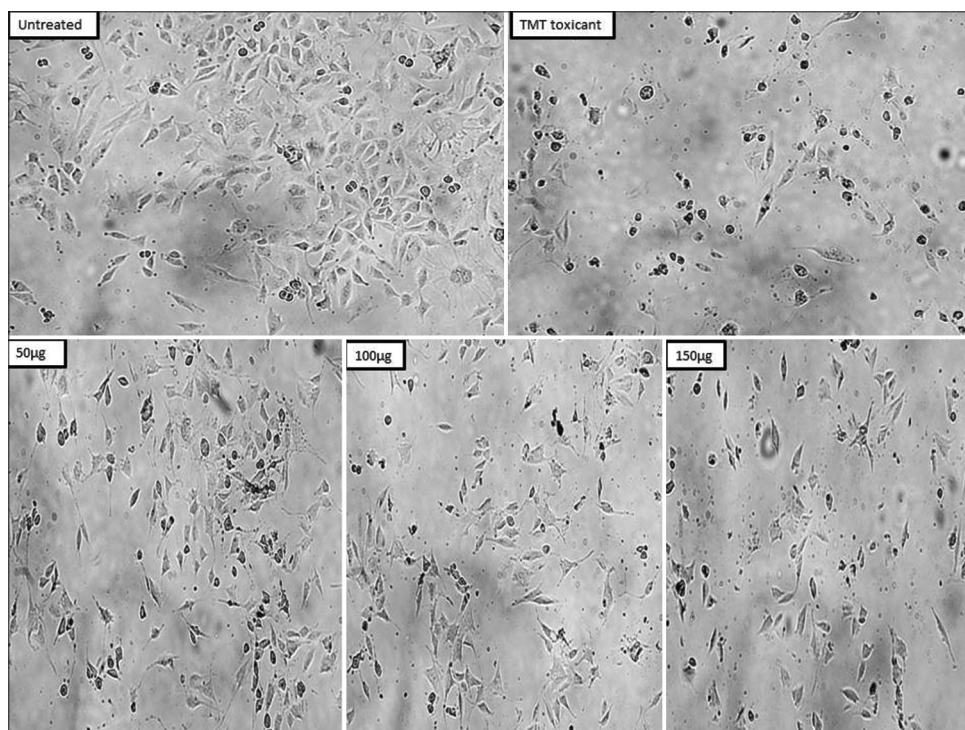


Figure 9: Morphological effects of gold nanoparticles on the SK-N-SH cell line

on the L929 fibroblast cell line, verifying the experimental data and supporting the conclusion that AuNPs have dose-dependent cytotoxicity.

In vitro neuro-protective activity on SK-N-SH cell line

The SK-S-NH neuroblastoma cell lines were used for the neuroprotective activity. Trimethyltin (TMT) was used as the

neurotoxicant. TMT-induced neurotoxicity primarily affects the limbic system and brainstem.^[36] The results revealed that the AuNPs had a significant ($P < 0.001$) neuroprotective efficacy against TMT-induced neurotoxicity in the SK-N-SH cell line. The percentage of cell viability reduced with increasing AuNPs concentration, demonstrating a dose-dependent impact [Table 5].

Table 4: Cytotoxicity of AuNPs on L929 fibroblast cell line

Treatments	Concentration $\mu\text{g/mL}$	Cell viability (%)
Cisplatin	15	6.97 \pm 0.0030
<i>F. arabica</i> AuNPs	50	92.08 \pm 0.0045
	100	80.83 \pm 0.0025
	150	69.06 \pm 0.0050
	200	56.14 \pm 0.0020
	250	27.81 \pm 0.0070

The data are represented as mean \pm standard error of the mean.
AuNPs: Gold nanoparticles

Table 5: Neuroprotective activity of gold nanoparticles

S. No.	Groups	Concentration ($\mu\text{g/mL}$)	Cell viability (%)
1	Neurotoxicant TMT (15 μg)	15	13.35 \pm 0.0060
2	Treatment group <i>F. arabica</i> -AuNPs+TMT	50	78.53 \pm 0.0055***
		100	60.73 \pm 0.0075***
		150	39.56 \pm 0.0095***

The data are provided as mean \pm standard error of the mean, $n=3$.
The results are statistically significant (*** $P<0.001$), and were determined using an unpaired t-test (two-tailed)

Morphological investigation under an inverted microscope showed that the cells in the normal control group were uniformly dispersed and elongated compared to the positive control (TMT-treated) cells, which had a high degree of morphological deformation, as well as damaged and dead cells. However, cell lines treated with *F. arabica* AuNPs displayed more viable cells with fewer dead, vesicle-shaped cells [Figure 9]. This observation suggests that the AuNPs have a protective effect on the neuroblastoma cells, potentially due to their antioxidant, anti-inflammatory, and neuroprotective properties.^[37]

CONCLUSION

The present investigation revealed the successful synthesis and characterisation of green-synthesized AuNPs from *F. arabica*, demonstrating their stability and optimum properties. The AuNPs' remarkable *in vitro* anti-inflammatory, COX-2 inhibitory, and antioxidant effects emphasize their potential for medicinal use. The AuNPs' biocompatibility was proven by their low toxicity on normal L929 cell lines, demonstrating their suitability for prospective medical applications. Furthermore, the neuroprotective potency observed in SK-N-SH cells against TMT-induced neurotoxicity highlights the nanoparticles' appealing significance in neurological disorders. Overall, the findings of this study open up novel avenues for the

use of *F. arabica*-synthesized AuNPs in neuroprotection, providing a potential strategy for developing therapeutics for neurodegenerative diseases. Future research should focus on exploring the mechanisms underlying these protective effects and evaluating the clinical efficacy of these nanoparticles in relevant models.

ACKNOWLEDGMENTS

The authors acknowledge and thank the Faculty of Pharmacy, Universiti Teknologi MARA (UiTM), Puncak Alam, Selangor, Malaysia, for providing support in this research. The authors would like to express sincere gratitude to Najran University, Najran, Saudi Arabia, and AlMaarefa University, Riyadh, Saudi Arabia, for supporting this research.

INSTITUTIONAL REVIEW BOARD STATEMENT

Not applicable.

INFORMED CONSENT STATEMENT

Not applicable.

DATA AVAILABILITY STATEMENT

All data have been presented in the manuscript.

REFERENCES

- Kumar A, Sidhu J, Lui F, Tsao JW. Alzheimer disease. In: StatPearls. Treasure Island, FL: StatPearls Publishing; 2025.
- 2024 Alzheimer's disease facts and figures. *Alzheimers Dement* 2024;20:3708-821.
- Fariás GA, Guzmán-Martínez L, Delgado C, Maccioni RB. Nutraceuticals: A novel concept in prevention and treatment of Alzheimer's disease and related disorders. *J Alzheimers Dis* 2024;42:357-67.
- Zhang J, Zhang Y, Wang J, Xia Y, Zhang J, Chen L. Recent advances in Alzheimer's disease: Mechanisms, clinical trials and new drug development strategies. *Signal Transduct Target Ther* 2024;9:211.
- Balakrishnan R, Azam S, Cho DY, Su-Kim I, Choi DK. Natural phytochemicals as novel therapeutic strategies to prevent and treat Parkinson's disease: Current knowledge and future perspectives. *Oxid Med Cell Longev* 2021;2021:6680935.
- Rahman MM, Islam MR, Akash S, Harun-Or-Rashid M, Ray TK, Rahaman S, *et al.* Recent advancements of

- nanoparticles application in cancer and neurodegenerative disorders: At a glance. *Biomed Pharmacother* 2022;153:113305.
7. Scarpa E, Cascione M, Griego A, Pellegrino P, Moschetti G, De Matteis V. Gold and silver nanoparticles in Alzheimer's and Parkinson's diagnostics and treatments. *Ibrain* 2023;9:298-315.
8. Singh GK. Medicinal properties and therapeutic potential of *Fagonia arabica* Linn: A comprehensive review. *Asian J Pharm* 2024;18:680-89.
9. Satpute R, Bhattacharya R, Kashyap RS, Purohit HJ, Deopujari JY, Tori GM, *et al.* Antioxidant potential of *Fagonia arabica* against the chemical ischemia-induced in PC12 cells. *Iran J Pharm Res* 2012;11:303-13.
10. Fatima H, Kainat A, Akbar F, Shinwari ZK, Naz I. Polarity guided extraction, HPLC based phytochemical quantification, and multimode biological evaluation of *Otostegialimbata* (Benth.) Boiss. *Arab J Chem* 2022;15:103583.
11. Shaikh JR, Patil MK. Qualitative tests for preliminary phytochemical screening: An overview. *Int J Chem Stud* 2020;8:603-8.
12. Aryal S, Baniya MK, Danekhu K, Kunwar P, Gurung R, Koirala N. Total phenolic content, flavonoid content and antioxidant potential of wild vegetables from western Nepal. *Plants (Basel)* 2019;8:96.
13. Zhishen J, Mengcheng T, Jianming W. The determination of flavonoid contents in mulberry and their scavenging effects on superoxide radicals. *Food Chem* 1999;64:555-9.
14. Hassanisaadi M, Bonjar GH, Rahdar A, Pandey S, Hosseini-pour A, Abdolshahi R. Environmentally safe biosynthesis of gold nanoparticles using plant water extracts. *Nanomaterials (Basel)* 2021;11:2033.
15. Tan F, Li T, Wang N, Lai SK, Tsoi CC, Yu W, *et al.* Rough gold films as broadband absorbers for plasmonic enhancement of TiO₂ photocurrent over 400–800 nm. *Sci Rep* 2016;6:33049.
16. Shojaei TR, Azhari S. Fabrication, functionalization, and dispersion of carbon nanotubes. In: *Emerging Applications of Nanoparticles and Architecture Nanostructures*. Netherlands: Elsevier; 2018. p. 501-31.
17. Rasmussen MK, Pedersen JN, Marie R. Size and surface charge characterization of nanoparticles with a salt gradient. *Nat Commun* 2020;11:2337.
18. Zheng J, Nagashima K, Parmiter D, de la Cruz J, Patri AK. SEM X-ray microanalysis of nanoparticles present in tissue or cultured cell thin sections. *Methods Mol Biol* 2011;697:93-9.
19. Sher A, Khalil AT, Dogan N, Ayaz M, Ahmad K. Valorization and repurposing of *Citrus limetta* fruit waste for fabrication of multifunctional AgNPs and their diverse nanomedicinal applications. *Appl Biochem Biotechnol* 2024;196:2067-85.
20. Singh P, Ahn S, Kang JP, Veronika S, Huo Y, Singh H, *et al.* *In vitro* anti-inflammatory activity of spherical silver nanoparticles and monodisperse hexagonal gold nanoparticles by fruit extract of *Prunus serrulata*: A green synthetic approach. *Artif Cells Nanomed Biotechnol* 2018;46:2022-32.
21. Alam W, Khan H, Saeed Jan M, Rashid U, Abusharha A, Daglia M. Synthesis, *in-vitro* inhibition of cyclooxygenases and *in silico* studies of new isoxazole derivatives. *Front Chem* 2023;11:1222047.
22. Baliyan S, Mukherjee R, Priyadarshini A, Vibhuti A, Gupta A, Pandey RP, *et al.* Determination of antioxidants by DPPH radical scavenging activity and quantitative phytochemical analysis of *Ficus religiosa*. *Molecules* 2022;27:1326.
23. Pillai RR, Sreelekshmi PB, Meera AP, Thomas S. Biosynthesized iron oxide nanoparticles: Cytotoxic evaluation against human colorectal cancer cell lines. *Mater Today* 2022;50:187-95.
24. Doggui S, Sahni JK, Arseneault M, Dao L, Ramassamy C. Neuronal uptake and neuroprotective effect of curcumin-loaded PLGA nanoparticles on the human SK-N-SH cell line. *J Alzheimers Dis* 2012;30:377-92.
25. Akintelu SA, Yao B, Folorunso AS. Bioremediation and pharmacological applications of gold nanoparticles synthesized from plant materials. *Heliyon* 2021;7:e06591.
26. Dhanasekar NN, Rahul GR, Narayanan KB, Raman G, Sakthivel N. Green chemistry approach for the synthesis of gold nanoparticles using the fungus *Alternaria* sp. *J Microbiol Biotechnol* 2025;25:1129-35.
27. Osman AI, Zhang Y, Farghali M, Rashwan AK, Eltaweil AS, ElMonaem EM, *et al.* Synthesis of green nanoparticles for energy, biomedical, environmental, agricultural, and food applications: A review. *Environ Chem Lett* 2024;22:841-87.
28. Kriegseis S, Vogl AY, Aretz L, Tonnesen T, Telle R. Zeta potential and long-term stability correlation of carbon-based suspensions for material jetting. *Open Ceramics* 2020;4:100037.
29. Aziz A, Shaikh H, Abbas A, Zehra KE, Javed B. Microscopic techniques for nanomaterials characterization: A concise review. *Microsc Res Tech* 2025;88:1599-614.
30. Javed R, Zia M, Naz S, Aisida SO, Ain NU, Ao Q. Role of capping agents in the application of nanoparticles in biomedicine and environmental remediation: Recent trends and future prospects. *J Nanobiotechnology* 2020;18:172.
31. Sivakavinesan M, Vanaja M, Annadurai G, Murugan AM, Salmen SH, Aljawdah HM. Antioxidant and anti-inflammatory activity of gold nanoparticles synthesized employing fruit peel extract of *Citrus sinensis* L. Osbeck. *Mater Res Express* 2024;11:105001.
32. Dhandapani S, Wang R, Cheol Hwang K, Kim H, Kim YJ. Exploring the potential anti-inflammatory effect of biosynthesized gold nanoparticles using *Isodon excisus* leaf tissue in human keratinocytes. *Arab J Chem* 2023;16:105113.
33. Abdallah BM, Ali EM. Therapeutic potential of green synthesized gold nanoparticles using extract

- of *Leptadenia hastata* against invasive pulmonary aspergillosis. *J Fungi (Basel)* 2022;8:442.
34. Nagalingam M, Kalpana VN, Rajeshwari VD, Panneerselvam A. Biosynthesis, characterization, and evaluation of bioactivities of leaf extract-mediated biocompatible gold nanoparticles from *Alternanthera bettzickiana*. *Biotechnol Rep (Amst)* 2018;19:e00268.
 35. Kus-Liśkiewicz M, Fickers P, Ben Tahar I. Biocompatibility and cytotoxicity of gold nanoparticles: Recent advances in methodologies and regulations. *Int J Mol Sci* 2021;22:10952.
 36. Liu Z, Lv J, Zhang Z, Wang B, Duan L, Li C, *et al.* The main mechanisms of trimethyltin chloride-induced neurotoxicity: Energy metabolism disorder and peroxidation damage. *Toxicol Lett* 2021;345:67-76.
 37. Chiang MC, Yang YP, Nicol CJ, Wang CJ. Gold nanoparticles in neurological diseases: A review of neuroprotection. *Int J Mol Sci* 2024;25:2360.

Source of Support: Nil. **Conflicts of Interest:** None declared.